EDITOR

P. GERSHOM JEBARAJ

CRYSTAL GROWTH AND CHARACTERIZATION

Indian Association for Crystal Growth

Crystal Growth and Characterization

Indian Association for Crystal Growth

Editor

P. Gershom Jebaraj
Life Member
Indian Association for Crystal Growth (IACG)

KOLKATA
PRESS BOOKS

FIRST EDITION, March 2022

DESIGN: TANIA KOLEY

ISBN: 978-81-955933-8-5

Publisher

KOLKATA PRESS BOOKS

CE-322, CHANDIBERIA, SHARODA POLLI,

KRISHNAPUR, KOLKATA-700102

PH: 9681708009 / 8777019179

http://kolkatapressbooks.com/

kolkatapressbooks@gmail.com

MRP: INR 400/-

CONTENTS

CHAPTER 5

A THEORETICAL INVESTIGATION OF BUMETANIDE USING CHARGE DENSITY AND TOPOLOGICAL PROPERTIES.

R.Niranjana Devi[1*] J.Kileyoba Vinnarasi[2] Poun Raj Parvonraja[3]

[1] Department of Physics, Fatima College, Madurai-625018.*
[2]PG and Research department of Chemistry, Thiagarajar College, Madurai.
[3]SSN Research Centre, Sri Sivasubramaniya Nadar College of Engineering, Chennai 603 110

5.1. INTRODUCTION

Hypertension or High Blood Pressure (HBP) is called a "silent killer" and it is a major cause of premature death worldwide and it affects between 16-37% of the population globally. Besides, 80% of all adults are at the risk from their blood pressure. A survey from the literature says that there are 234 million Indian adults are affected with hypertension which is expected to be the large increase in cardiovascular diseases burden in near future. HBP can lead to many serious health problems, such as heart attack, heart failure, stroke, and kidney disease. Treating high blood pressure early is important in preventing these problems. Moreover dozens of different medications can help to treat high blood pressure. These drugs are called anti-hypertensives. One such potent anti-hypertensive drug candidate is Bumetanide. Bumetanide (BMT) also known as Bumex is highly useful in the treatment of swelling and high blood pressure. This is a loop diuretic and works by decreasing the re-absorption of sodium by the kidneys [1,2]. It works by blocking the cation-chloride co-transporter NKCC1 (membrane transport protein, Na–K–Cl), which further decreases chloride concentration in neurons and therefore intensifying the inhibitory effect of GABA (γ-aminobutryic acid). GABA is known as a chief inhibitory neurotransmitter in the central nervous system. It is directly accountable for muscle tone. This mechanism of action helps Bumetanide to act as a potential anti-seizure drug [3].

This study about Bumetanide in the view point of structural, topological, reactivity and interaction properties will give rich information which further enables pharmacologists and drug engineers to design new drugs with reduced side effects and improved efficiency

5.2. THEORETICAL CALCULATIONS

5.2.1. Geometry Optimization

In this work geometry optimization of Bumetanide ($C_{17}H_{20}N_2O_5S$) was done at the ground state level using Becke-3-Lee-Yang-Parr hybrid exchange functional (B3LYP) of the density functional theory with 6311G(d, p) basis sets using GAUSSIAN 09W software [4].

Generally, geometry optimization tries to locate minima on the potential energy surface, and is a mathematical relationship connecting molecular structure and the resultant energy. The target molecule has 45 atoms and it has 129 degrees of freedom.

5.3. RESULTS AND DISCUSSION

5.3.1. Structural Aspects

The structure of the molecule Bumetanide has two rings connected by an oxygen atom. The optimized structure of Bumetanide was shown in figure 5.1. The bond length range (1.373Å-1.540Å) of the C-C bonds suggests that they all have single bond except C17-C18 which has double bond and the value is found to be 1.373Å. The C3 atom has three bonds with neighboring atoms which also has the C2-C3-C4, C2-C3-O12 and C3-C4-O12 plane angles 119.99°, 120.01° and 119.99° respectively which show the sp2 hybridization and trigonal planar geometry for the central carbon atom. The bond length and bond angle values of the molecule BMT has been given in Table 5.1 and 5.2 respectively.

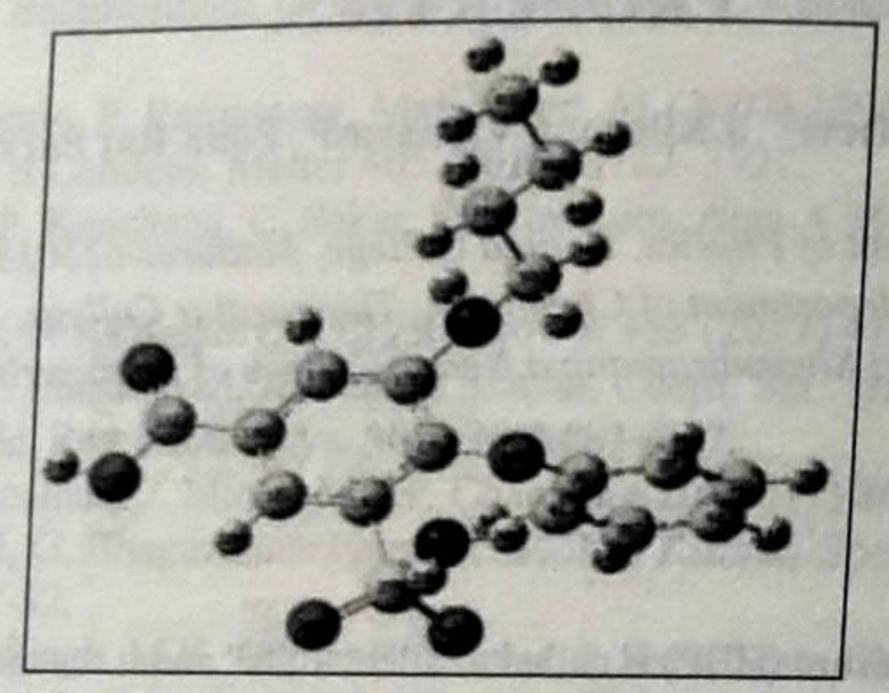

Figure 5.1 The Optimized structure of Bumetanide molecule.

Table 5.1 Bond Lengths of Bumetanide molecule

Bonds	Bond Length (Å)	Bonds	Bond Length (Å)
C1-C2	1.395	C16-H20	1.070
C1-C6	1.395	C17-H19	1.100
C1-C7	1.100	C33-H34	1.070
C2-C3	1.395	C33-H35	1.070
C2-C8	1.100	C36-H37	1.070
C3-C4	1.395	C36-H38	1.070
C4-C5	1.395	C39-H40	1.070
C5-C6	1.395	C39-H41	1.070
C13-C14	1.422	C42-H43	1.070
C13-C15	1.373	C42-H44	1.070
C14-C16	1.419	C42-H45	1.070
C15-C17	1.416	C3-O12	1.430
C16-C18	1.422	C13-O12	1.430
C17-C18	1.373	C21-O22	1.230
C18-C21	1.540	C21-O23	1.357
C33-C36	1.540	O23-H24	0.971
C36-C39	1.540	C14-S25	1.780
C39-C42	1.540	S25-O26	1.396

C15-N31	1.470	S25-O27	1.396
C33-N31	1.470	S25-N28	1.710
C4-H9	1.100	N28-H29	1.000
C5-H10	1.100	N28-H30	1.000
C6-H11	1.100	N31-H32	1.000

Table 5.2 Bond angles of Bumetanide molecule

Bonds	Bond angle (°)	Bonds	Bond angle (°)	Bonds	Bond angles (°)
C1-C2-C3	120.01	C6-C1-H7	120.00	C3-O12-C13	109.50
C1-C6-C5	120.00	C6-C5-H10	119.98	C4-C3-O12	119.99
C2-C1-C6	120.00	C14-C16-H20	120.47	C13-C14-S25	120.40
C2-C3-C4	119.99	C15-C17-H19	118.98	C14-S25-O26	110.10
C3-C4-C5	119.99	C18-C17-H19	120.65	C14-S25-O27	110.10
C4-C5-C6	120.00	C18-C16-H20	120.47	C14-S25-N28	93.80
C13-C14-C16	119.20	C33-C36-H37	109.47	C15-N31-H32	109.47
C13-C15-C17	120.32	C33-C36-H38	109.47	C15-N31-C33	109.47
C14-C13-C15	120.50	C36-C39-H40	109.47	C16-C14-S25	120.40
C14-C16-C18	119.06	C36-C39-H41	109.47	C18-C21-O22	130.07
C15-C17-C18	120.37	C39-C42-H43	109.47	C18-C21-O23	112.29
C16-C18-C17	120.55	C39-C42-H44	109.47	C21-O23-H24	110.61
C16-C18-C21	118.59	C39-C42-H45	109.47	O12-C13-C14	118.64
C17-C18-C21	120.86	H34-C33-C36	109.47	O12-C13-C15	120.86
C33-C36-C39	109.47	H35-C33-C36	109.47	O22-C21-O23	117.63
C36-C39-C42	109.47	H37-C36-C39	109.47	O26-S25-O27	119.60
C13-C15-N31	120.69	H38-C36-C39	109.47	O26-S25-N28	110.10
C17-C15-N31	118.99	H40-C39-C42	109.47	O27-S25-N28	110.10
C1-C2-H8	119.98	H41-C39-C42	109.47	S25-N28-H29	109.47
C1-C6-H11	120.01	H34-C33-H35	109.47	S25-N28-H30	109.47
C2-C1-H7	120.00	H37-C36-H38	109.47	H29-N28-H30	109.47
C3-C2-H8	120.01	H40-C39-H41	109.47	H32-N31-C33	109.47
C3-C4-H9	119.98	H43-C42-H44	109.47	N31-C33-H34	109.47
C4-C5-H10	120.01	H43-C42-H45	109.47	N31-C33-H35	109.47
C5-C4-H9	120.02	H44-C42-H45	109.47	N31-C33-C36	109.47
C5-C6-H11	119.99	C2-C3-O12	120.01		

5.3.2. Intra and Inter Molecular Interactions

The intermolecular interactions of the molecule with the neighbouring molecules can be explained and picturized by the Hirshfeld analysis and finger print plot [5, 6]. The distance from the Hirshfeld surface to the nearest atoms outside and inside the surface are characterized by the quantities d_e and d_i and the normalized contact distance d_{norm}. The 3D Hirshfeld plot and 2D finger print plot have been given in Figure 2a and 2b. The large and deep red circular patches on the 3 dimensional Hirshfeld surface points out the close contact interactions responsible for hydrogen bond contacts (O-H…O) and the light red spots on the surfaces represent C-H…π interactions. The strength of the O-H….O interaction is seen by the red colour spots. The O…H/H…O inter molecular interactions are seen as distinct spikes in the fingerprint plot. Sets of diffuse points between the spikes are from H…H contacts and they play a major role which has the contribution of 53.7% in the packing of the molecule in the crystal.

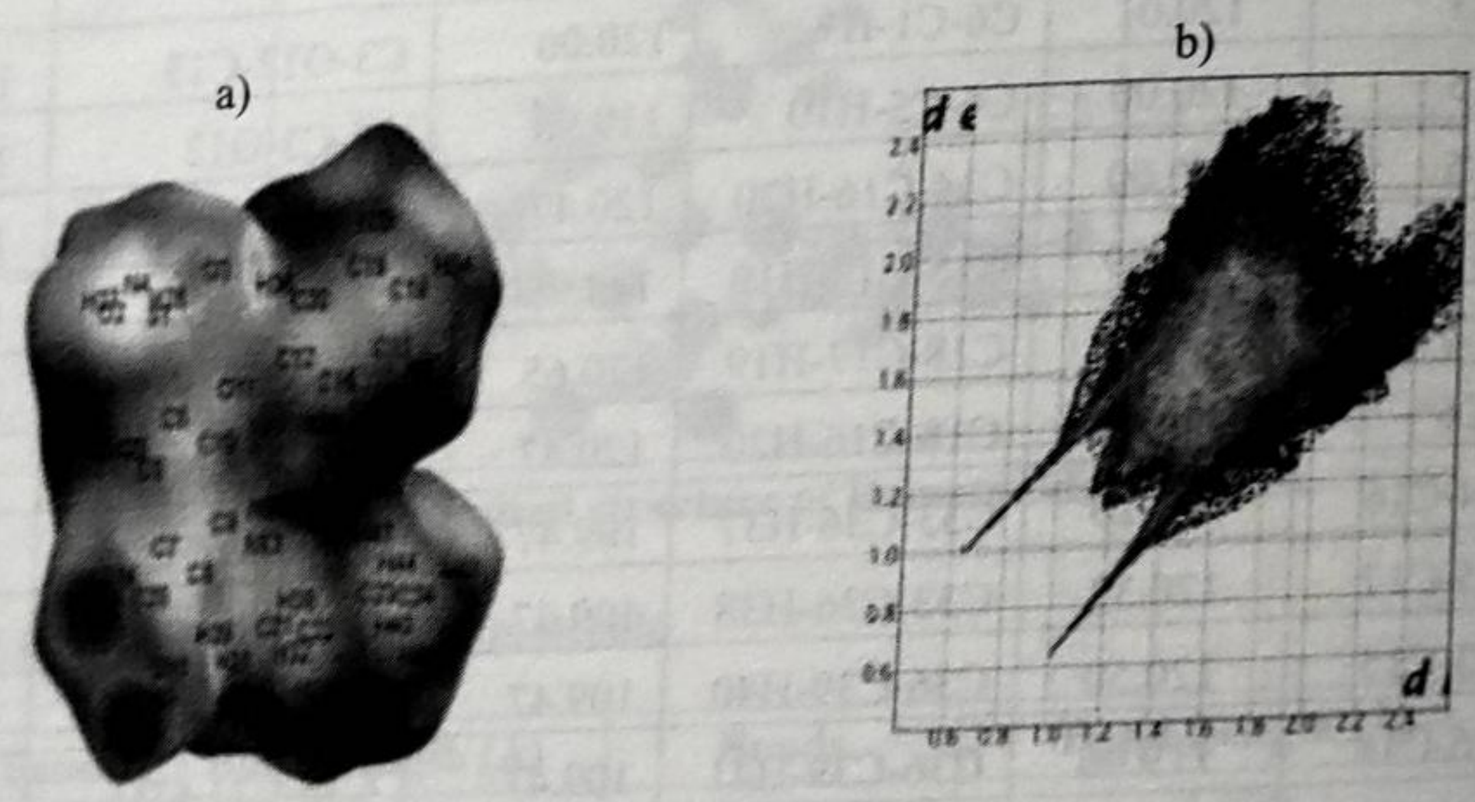

Figure 5.2 a) Hirshfeld plot and b) Finger print plot of the molecule.

5.3.3. Topological Properties

AIM topological analysis was carried out with the help of *Multiwfn 3.3.9* [7]. Bader's AIM theory [8] is used as a great tool for the qualitative analysis of the electron density $\rho(r)$ and Laplacian $\nabla^2\rho(r)$ of the electron density. Within the AIM theory, the topology of the electron density is exposed by its gradient vector field. The nucleus is known as an attractor and the paths converging to a nucleus represents a region of space known as atomic basin. Some gradient paths reaching a nucleus do not start from infinity but from a point in between two nuclei which is called a Bond Critical Point (BCP) where the gradient of $\rho(r)$ vanishes.

The topological properties of the electron density are listed in table 5.3. The range of electron density for the C-C bonds 1.613 e/Å^3 - 2.085e/Å^3 in which the C1-C2, C1-C6, C5-C6, C14-C16 and C17-C18 bonds has the same electron density value of 2.085 e/Å^3. The molecular graph showing the critical point between the atoms is shown in figure 5.3 a. The regions of charge concentration and charge depletion can be viewed through the positive and negative Laplacian of the electron density values. Charges are highly concentrated in the bonding region (Figure. 3b). Among all the bonds, the O12-N28 and O12-H35 bonds are having positive Laplacian values (0.96 e/Å^5 and 1.20 e/Å^5) which show the closed shell interaction of the bonds. The plot of electron localization function [9] clearly shows the sharing of electrons between the atoms in the bond path and also the lone pair details of the O12 atom (Figure.3c).

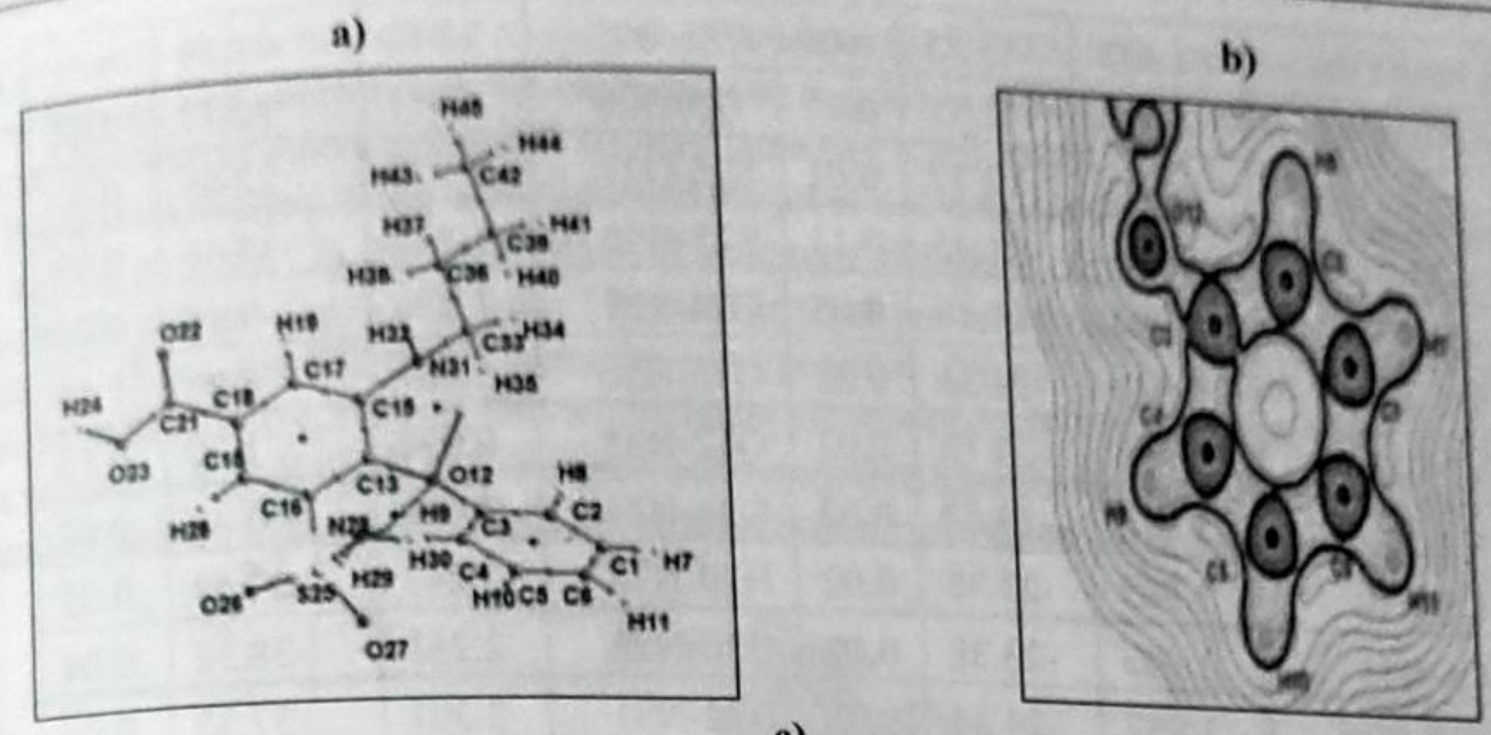

Figure 5.3: a) Molecular graph b) Laplacian of the electron density c) Electron localization function of the Bumetanide molecule.

Table 5.3 Topological properties of the Bumetanide molecule.

Bonds	ρ (e/Å^3)	$\nabla^2\rho$ (e/Å^5)	ε	Bonds	ρ (e/Å^3)	$\nabla^2\rho$ (e/Å^5)	ε
C1-C2	2.085	-20.72	0.21	C17-H19	1.910	-23.62	0.02
C1-C6	2.085	-20.72	0.2	C33-H34	1.890	-22.89	0.03
C2-C3	2.112	-21.45	0.25	C33-H35	1.917	-23.62	0.03
C3-C4	2.112	-21.21	0.24	C36-H37	1.836	-21.45	0
C4-C5	2.078	-20.48	0.21	C36-H38	1.849	-21.93	0
C5-C6	2.085	-20.72	0.2	C39-H40	1.849	-21.93	0.01
C13-C14	2.078	-20.48	0.28	C39-H41	1.849	-21.69	0.01
C13-C15	2.031	-19.76	0.27	C42-H44	1.842	-21.93	0.01
C14-C16	2.085	-20.48	0.21	C42-H43	1.842	-21.69	0.01
C15-C17	2.065	-20.24	0.22	C42-H45	1.842	-21.69	0.01
C16-C18	2.072	-20.48	0.2	C3-O12	1.728	-5.99	0.02
C17-C18	2.085	-20.72	0.21	C13-O12	1.856	-9.16	0.01
C18-C21	1.802	-15.39	0.13	C21-O22	2.814	-5.06	0.08

C33-C36	1.633	-13.25	0.04	C21-O23	2.018	-12.29	0.01
C36-C39	1.620	-12.77	0.01	S25-O26	1.971	22.17	0.04
C39-C42	1.613	-12.77	0.01	S25-O27	1.971	22.65	0.01
C15-N31	2.038	-21.45	0.11	S25-N28	1.545	-14.46	0.09
C33-N31	1.701	-15.18	0.03	C14-S25	1.356	-9.16	0.06
C1-H7	1.903	-23.38	0.02	O12-N28	0.061	0.96	1.42
C2-H8	1.890	-23.13	0.02	O12-H35	0.094	1.20	0.16
C4-H9	1.910	-23.62	0.02	O23-H24	2.429	-60.49	0.02
C5-H10	1.903	-23.38	0.02	H29-N28	2.247	-37.59	0.05
C6-H11	1.903	-23.38	0.02	H30-N28	2.261	-38.32	0.04
C16-H20	1.937	-24.34	0.02	H32-N31	2.301	-37.35	0.06

5.3.4. Chemical Reactivity

The highest occupied molecular orbital (HOMO) and lowest unoccupied molecular orbital (LUMO) are the two important molecular orbitals. The HOMO represents the ability to donate an electron which has π character and the LUMO with π^* character has the capability to accept an electron. The HOMO and LUMO energies were calculated by the standard basis set B3LYP/6-311G++ (d, p) (5D, 7F) where HOMO state is found at -0.231eV and LUMO is found at -0.069eV. The DFT method predicts that the HOMO – LUMO energy gap of BMT is 0.087eV which is found to be very low and it leads to less stability of the molecule and pronounces the softness of the molecule.

Table 5.4: Reactivity properties of the Bumetanide molecule.

Molecular descriptor	Energy (a.u.) HCTZ
Electron affinity $A=[-E_{LUMO}]$	0.069
Ionization potential $I=[-E_{HOMO}]$	0.231
Global hardness $\eta=(I-A)/2$	0.081
softness $S=1/\eta$	12.392
Electronegativity $\chi=(I+A)/2$	0.150
Electrophilicity index $\omega=\mu^2/2\eta$	0.139

On the basis of the density functional theory the ionization Potential, electron affinity, hardness, softness, electronegativity and the electrophilicity index are calculated and tabulated in Table 5.4. The values help us to characterize the molecule that this molecule is chemically reactive, less toxic and soft molecule.

5.3.5. Electrostatic Properties

The molecular electrostatic potential helps to identify the site and chemical reactivity of the molecule [10]. Nucleophilic regions (δ-)(prone to electrophilic attack) are found near O atoms and electrophilic regions(δ+) (prone to nucleophilic attack) are found near H atoms and remaining other atoms. The electrostatic potential map of the molecule BMT is shown in Figure.4.

This map evidently shows that all the oxygen atoms such as O12, O22, O23, O26 and O27 are electron rich sites where they all can interact with the electron poor regions in the target protein. It can be a good polar molecule as the value of dipole moment is slightly large (μ= 4.86Debye).

Population analysis is the unembellished model in order to describe charge distribution and also for deriving atomic charges. In the application of quantum chemical calculation to molecular systems, the Mulliken atomic charges play a vital role. The AIM charges are based upon the electron density values. The Among all the atoms, the S25 atoms bears the most positive charge (AIM: 2.806e, MPA: 1.081e) and the O26 atom through AIM (-1.270e) MPA(-0.47e) bears the most negative charge. The MPA and AIM charges are listed in table 5.5. All the N and O atoms bears negative charges in both the schemes and the schemes clearly predict that the O26 atom possess the more electron rich region among all the O atoms.

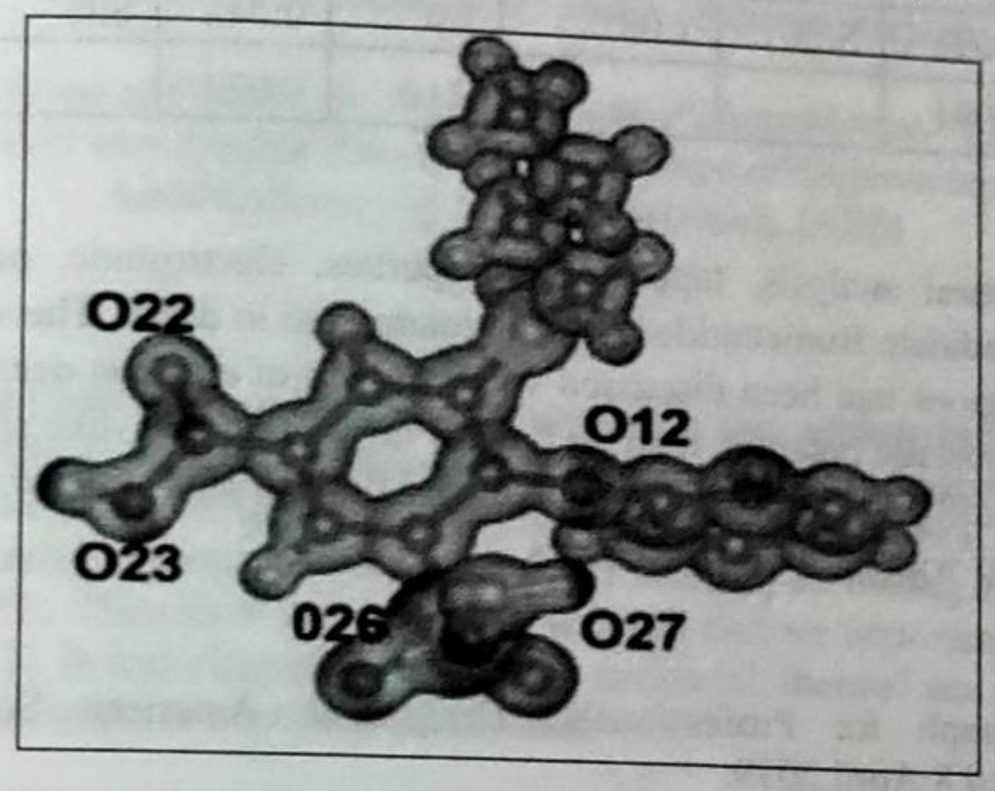

Figure 5.4: Molecular electrostatic potential map of Bumetanide molecule.

Table 5.5 MPA and AIM charges of Bumetanide molecule.

Atoms	Q(e) MPA	Atoms	Q(e) MPA	Atoms	Q(e) AIM	Atoms	Q(e) AIM
C1	-0.093	H11	0.092	C1	-0.003	H11	0.018
C2	-0.088	H19	0.142	C2	0.001	H19	0.060
C3	0.165	H20	0.132	C3	0.426	H20	0.111
C4	-0.067	H24	0.267	C4	0.018	H24	0.584
C5	-0.08	H29	0.261	C5	0.003	H29	0.399
C6	-0.102	H30	0.261	C6	-0.010	H30	0.401
C13	0.274	H32	0.221	C13	0.504	H32	0.347
C14	-0.323	H34	0.131	C14	-0.122	H34	0.005
C15	0.051	H35	0.119	C15	0.402	H35	0.030
C16	0.096	H37	0.109	C16	0.019	H37	-0.028
C17	0.054	H38	0.136	C17	-0.006	H38	-0.012
C18	-0.237	H40	0.111	C18	0.003	H40	-0.021
C21	0.414	H41	0.11	C21	1.515	H41	-0.022

C33	-0.038	H43	0.108	C33	0.353	H43	-0.010
C36	-0.293	H44	0.106	C36	0.043	H44	-0.007
C39	-0.232	H45	0.106	C39	0.061	H45	-0.012
C42	-0.284	O12	-0.36	C42	0.031	O12	-1.096
N28	-0.606	O22	-0.347	N28	-1.130	O22	-1.139
N31	-0.497	O23	-0.341	N31	-1.017	O23	-1.083
H7	0.095	O26	-0.47	H7	0.020	O26	-1.270
H8	0.099	O27	-0.47	H8	0.027	O27	-1.261
H9	0.093	S25	1.081	H9	0.042	S25	2.806
H10	0.094			H10	0.023		

5.4. CONCLUSION

In this study, the structural analysis, topological properties, electrostatic, nature, reactivity and interaction of the drug candidate Bumetanide had been interpreted in detail. The strength of the bonds, electron rich and poor regions had been discussed with the help of electron density, Laplacian of the electron density and electrostatic potential map. It has the favourable drug-like properties such as high chemical reactivity, very soft and less toxicity. This study will pave path way for the drug engineers to design more efficacy drugs with reduced side effects.

REFERENCES

1. Bumetanide Monograph for Professionals" Drugs.com. American Society of Health-System Pharmacists. Retrieved 8 April 2019.
2. British national formulary: BNF 76 (76 ed.). Pharmaceutical Press. 2018. pp. 225–225. ISBN 9780857113382.
3. W. Löscher, M. Puskarjov, and K. Kaila (2013). "Cation-chloride cotransporters NKCC1 and KCC2 as potential targets for novel antiepileptic and antiepileptogenic treatments," Neuropharmacology 69, 62–74.
4. M.J. Frisch, G.W. Trucks, H.B. Schlegel, G.E. Scuseria, M.A. Robb, J.R. Cheeseman etal., Gaussian, Inc., Wallingford CT, 09, Gaussian Revision C.01, Gaussian, Inc. 340 Quinnipiac St., Bldg. 40, Wallingford CT 06492 (2010).
5. J.J. McKinnon, M.A. Spackman, A.S. Mitchell. Acta Cryst., (2004) B60 , 627.
6. S.K. Wolff, D.J. Grimwood, J. McKinnon, D. Jayatilaka and M.A. Spackman,
1. CrystalExplorer3.0. University ofWestern Australia, Perth, (2007)
7. Lu, Tian & Chen, Feiwu. (2012). Multiwfn: A multifunctional wavefunction analyzer. Journal of computational chemistry. 33. 580-92. 10.1002/jcc.22885.
8. R.F. Bader, Atoms in Molecules-A Quantum Theory. Clanderon Press, Oxford (1990)
9. A. D. Becke and K. E. Edgecombe, J. Chem. Phys., (1990), 92, 5397–5403.
10. H.J. Bohm, G. Schneider, Protien-Ligand Interactions: From Molecular Recognition to Drug Design. John Wiley and Sons (2003).

Shri. P. Gershom Jebaraj did his schooling in Ambrose Higher Secondary School, Meignanapuram. He did B.Sc Physics in Aditanar College of Arts and Science, Tiruchendur and he was selected as the Best Outgoing Student. He also won National Award from Department of Atomic Energy, Mumbai. He did M.Sc. Physics and M.Phil. Physics in Manonmaniam Sundaranar University, Tirunelveli. He got **First Rank** in M.Sc and received **Gold Medal** from the former Governor of Tamilnadu Dr. Rama Mohan Rao. He has presented many research papers in the field of Physics and Education in National/International Seminars and Conferences. His research papers were published in reputed Journals and refereed Conference Proceedings. He also attended various training courses and workshops such as "UGC Sponsored orientation Course for College Teachers", "Workshop on Student Counseling" and **"NSS Officers Training"** conducted by Ministry of Sports and Youth Affairs, Government of India. He Qualified State Eligibility Test (SET) in the Subject Physics. He has already published **"Engineering Physics-I"**, **"Engineering Physics-II"** and **"Experimental Engineering Physics"** Text Books for First Year B.E. & B. Tech Students of Anna University, Tamilnadu.

He is the Life Member of

- Indian Physics Association (IPA)
- Indian Society for Technical Education (ISTE)
- All India Association for Educational Research (AIAER)
- Indian Association for Crystal Growth (IACG)
- Indian Society for Radiation Physics (ISRP)
- Indian Academicians and Researchers Association (IARA).

KOLKATA
PRESS BOOKS
Ph: 9681708009 / 8777019179

ISBN: 978-81-955933-8-5

9 788195 593385

MRP: ₹400/-